

# Ship Detection in SAR Image Based on Information Geometry Method

Xiangxiang Yang<sup>1</sup>, Meng Yang<sup>1, \*</sup>, Yinhua Zhang<sup>1</sup>, and Gong Zhang<sup>2</sup>

**Abstract**—Aiming at the problem of high false alarm rate with respect to adaptive threshold in the ship detection from synthetic aperture radar (SAR) images, a novel strategy increasing robustness when using local adaptive threshold is proposed. In this article, we establish a fusion detection model based on a combination of the information geometry and surface geometry. Information geometry from a metric viewpoint can increase the contrast between targets and clutter in SAR image. Local surface feature gives a brief application of adaptive threshold method in ship detection from SAR images by means of the constant false-alarm-rate. Experiments indicate that the proposed geometry-based approach can effectively detect ship targets from complex background SAR images by using the method of fusion processing.

## 1. INTRODUCTION

Synthetic aperture radar (SAR) is an active remote sensor, which has all-time and all-weather observing ability and total global coverage. The use of SAR provides an effective way to monitor ships, which encompass traffic surveillance, maritime security, fishing activity control, and even island dispute resolving [1]. With the increase of the resolution of SAR images, it becomes more and more important to improve and automate detection and identification of suspicious or non-collaborative ships, facilitating decision making, and reducing the response time of authorities [2]. Ship detection belongs to the category of SAR image processing. It is the main issue for detection that the test statistic should be constructed and evaluated properly in SAR target detection. Also, the principle of ship detection in SAR image uses different statistical and geometrical features of ship targets and sea clutter. Ship detection from SAR images has been studied extensively, and many ship target detection methods have been developed, such as global and local adaptive threshold algorithms [3].

Global threshold algorithms search for SAR bright objects by using a global threshold. Any pixel intensities above the global threshold are declared as targets of interest. Most of these algorithms use statistical methods, such as Bayesian detectors, likelihood ratio detectors, moment detectors, entropy detectors, and multiscale histogram detectors. SAR imaging is dependent on many factors, such as corner reflections and multiple reflections from the ship and sea surface. Because of the diversity and complexity of such factors, local adaptive threshold algorithms are the most common detection methods for ship detection in SAR images.

Adaptive threshold algorithms are designed to look for pixels that use different thresholds according to the region under consideration [4]. Among these, constant false alarm rate (CFAR) algorithm is the most commonly used and most effective detection algorithm in SAR detection field [5]. It has low computational complexity and adaptive threshold preserving constant false alarm probability by using the given background clutter distribution model and false alarm rate. However, complicated sea

---

*Received 1 January 2019, Accepted 15 February 2019, Scheduled 21 February 2019*

\* Corresponding author: Meng Yang (yangmeng@hdu.edu.cn).

<sup>1</sup> College of Communication Engineering, Hangzhou Dianzi University, Hangzhou 310018, China. <sup>2</sup> Key Laboratory of Radar Imaging and Microwave Photonics (Nanjing University of Aeronautics and Astronautics), Ministry of Education, Nanjing 210016, China.

conditions cause the high nonhomogeneity of sea clutter in the SAR images, which affect the CFAR-based automatic target detection [6]. Moreover, they often rely on a size parameter which may change for different images, providing, in some cases, too cluttered results.

Information geometry emerged from the study of intrinsic properties of manifolds of probability distributions [7]. In other words, this theory is a combination of mathematical statistic models and geometrical analysis methods. With the development of geometrical analysis method and numerical technique, it widens the applicability of information geometry to signal/image analysis and optimal design. One purpose of this research was to get better understanding and analysis of statistical manifold and its geometric structure in parameter space. Based on the information geometry and surface manifold theory, this work aims to explore its application in ship detection from SAR images and to analyze the detection problems in this field with a new perspective [8].

In this work, one principal tool is to construct the manifold of distributional class based on information geometry and give its geometric structure, such as the Fisher metric matrix, connection coefficients, and curvature tensors. From the viewpoint of geometry, the aim of this study is to show the benefits of statistical manifolds and geometrical surface suitable for ship detection in SAR imagery. Statistical manifolds represent smooth families of probability density functions. Geometrical surface is used to represent SAR image. They allow geometrical features to be applied to problems in ship target detection of SAR images.

The main contributions in the proposed method are as follows: 1) curvature tensors construction for statistical manifold with high performance are exploited based on information geometry, 2) fusion of statistical and geometrical features is used to exploit the microstructure features of SAR images.

## 2. FUSION DETECTION TECHNIQUE

We can unify many of the questions in a very elegant geometric way which usually yields additional insight and understanding. This study investigates a fusion detection frame based on information geometry. By utilizing geometric structures, the designed detector can be applied to ship detection in complex clutter background.

This section deals with certain features of image, including statistical feature and surface feature, where definition and analysis involve geometrical structures. We begin with a basic discussion of geometric structure of Gamma manifold, followed by an introduction to surface feature. Then, we consider the combination of statistical feature and surface feature. Fig. 1 describes the framework for the ship detection procedure.

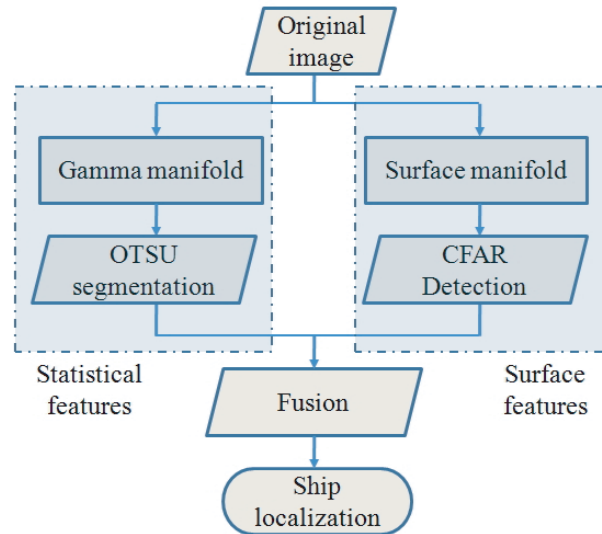


**Figure 1.** Framework of the proposed method for ship detection.

### 2.1. Statistical Feature

The differential-geometric structure of the set of positive densities on a given measure space has raised the interest of many researchers after the discovery of the geometric meaning of the Fisher information metric which defines a Riemannian metric uniquely.

Many important families of probability distributions are Riemannian manifold equipped with Fisher information metric. The first step is to define a Riemannian manifold which is the adaptation of a proper positive density to model the sea clutter in SAR image. Gamma distribution has been, until now, frequently used for the modeling of intensity of SAR imagery. It is also proved that, in most cases, the Gamma distribution outperforms some of parametric models (such as Lognormal distribution and Weibull distribution) in terms of modeling of intensity of SAR imagery.

Without loss of generality, we restrict our method to the case of two-parameter Gamma distribution in this article. The probability density function of Gamma distribution is defined by [9]

$$f(x) = \frac{1}{\gamma\Gamma(\kappa)} \left(\frac{x}{\gamma}\right)^{\kappa-1} \exp\left(-\frac{x}{\gamma}\right) \quad x \geq 0 \tag{1}$$

where  $\kappa$  and  $\gamma$  denote the shape and scale parameter respectively, and  $\Gamma$  denotes the gamma function.

Let  $\nu = \gamma^{-1}$ . Then, the probability density function can be written as the form

$$f(x) = \frac{\nu^\kappa}{\Gamma(\kappa)} x^{\kappa-1} \exp(-\nu x) \tag{2}$$

The logarithm of  $f(x)$  has the form

$$\log f(x) = [(\kappa - 1) \log x - \nu x] - [\log \Gamma(\kappa) - \kappa \log \nu] \tag{3}$$

So, corresponding potential function is defined by

$$\phi(\nu, \kappa) = \log \Gamma(\kappa) - \kappa \log \nu \tag{4}$$

We consider two-dimensional manifold according to Riemannian geometry theory. Taking the coordinate  $(\theta_1, \theta_2) = (\nu, \kappa)$ . Set  $\partial_i = \frac{\partial}{\partial \theta_i}$  ( $i = 1, 2$ ), which are the coordinate vector fields in a local chart. The Fisher metric  $[g_{ij}]$  is given with respect to coordinates  $(\theta_1, \theta_2)$  [10].

$$[g_{ij}] = [\partial_{ij}^2 \phi(\nu, \kappa)] \tag{5}$$

The Riemannian metric  $g$  can be obtained by direct calculation

$$g = [g_{ij}] = \begin{bmatrix} \frac{\kappa}{\nu^2} & -\frac{1}{\nu} \\ -\frac{1}{\nu} & \frac{d^2}{d\kappa^2} \log \Gamma(\kappa) \end{bmatrix} \tag{6}$$

Consider the metric connection  $\nabla$  with respect to Riemannian metric  $g$  on the Gamma manifold. Then,  $\nabla$  satisfies Eq. (7), for all vector fields  $X = X_i \partial_i$ ,  $Y = Y_i \partial_i$ , and  $Z = Z_i \partial_i$ ,

$$Zg(X, Y) = g(\nabla_Z X, Y) + g(X, \nabla_Z Y) \tag{7}$$

Using the coordinate expressions, we get

$$\partial_k g_{ij} = \Gamma_{ki}^l g_{lj} + \Gamma_{kj}^l g_{li} \tag{8}$$

where  $\Gamma_{ki}^l$  and  $\Gamma_{kj}^l$  denote the connection coefficients of  $\nabla$ . Let

$$\Gamma_{ij,k} \triangleq \Gamma_{ij}^l g_{lk} \tag{9}$$

and we have

$$\Gamma_{ij,k} = \frac{1}{2} (\partial_i g_{jk} + \partial_j g_{ki} - \partial_k g_{ij}) \tag{10}$$

If a Riemannian metric is given in local coordinates by  $g$ , the curvature tensor is given by

$$R_{ijk}^l = \partial_i \Gamma_{jk}^l - \partial_j \Gamma_{ik}^l + \sum_h \left( \Gamma_{jk}^h \Gamma_{ih}^l - \Gamma_{ik}^h \Gamma_{jh}^l \right) \tag{11}$$

By direct calculation, the curvature tensor of the generalized Gamma distribution manifold is given by

$$R_{121}^2 = \frac{\psi'(\kappa) + \kappa\psi''(\kappa)}{4\nu^2 [1 - \kappa\psi'(\kappa)]} \quad (12)$$

where  $\psi(\kappa)$  denotes the digamma function.

For each image patch of the 2-D SAR image  $I$ , with a size of  $h$ -by- $h$ , Riemannian curvature tensor  $R_{121}^2$  at position  $(i, j)$  is calculated. We reshape curvature tensors of surface into matrix  $I_1'$ . The maximum between-class variance method (OTSU method) [11] is implemented to locate regions of interest (ROIs). The detected result is denoted by  $I_1''$ .

## 2.2. Surface Feature

In the previous subsection, a statistical manifold method based on gray statistical characteristic of SAR image was presented. In fact, an image, a set of two-dimensional data, can be treated as a surface in three-dimensional space. From this point of view, it is necessary to smooth the speckle of SAR image while preserving the radar target scattering characteristics.

For the first step, a reasonable filtering is needed for SAR image. The object of the filtering is to preserve the target information and to filter out most clutter information. Because the nonlinear anisotropic diffusion filtering has shown the good property of smoothing noise while preserving the accuracy of edges, it has been widely used in image processing. In this work, the nonlinear anisotropic diffusive process, suitable for distributed parallel computing, has been used to obtain a “surface”, viewed abstractly, a two-dimensional manifold in contemporary differential geometry.

Diffusion techniques in image filtering are based on the well-known diffusion equation [12].

$$\frac{\partial}{\partial t} I^t(i, j) = \text{div}[D^t(i, j)\nabla I^t(i, j)] \quad (13)$$

with initial condition  $I^0(i, j) = I(i, j)$ .  $I^t(i, j)$  denotes the grey value at position  $(i, j)$ , and  $t$  denotes the iteration time.  $\text{div}$  and  $\nabla$  denote the divergence and gradient operators respectively, and  $D^t$  is a symmetric positive definite tensor which depends on the local structure of  $I^t$ ,

$$D^t(i, j) = \frac{1}{\sqrt{\left(\|\nabla(G_\sigma * I)\|^2 + \eta^2\right)^\tau}} \quad (14)$$

where  $\tau \in (1, 2)$ ,  $*$  denotes the convolution operation,  $G_\sigma$  a Gaussian filter, and  $\eta > 0$  the conductance parameter. We denote the filtered image as  $I_2'$ , where the speckle filter not only is adaptive but also takes account of the different image structure between object and background.

After smoothing out the sea clutter, local adaptive threshold algorithm is designed to search for pixel values which are unusually bright compared to those in the surrounding area. Among local adaptive threshold algorithms, CFAR method is mainly used in SAR target detection. Usually, the commonly used CFAR detectors are based on assumptions about the background statistics which do not include the changes speckle filtering brings about, but they are suitable (in practice) for speckle filtered imagery. This is because even if the adopted detectors are not CFAR for the true background distribution of the SAR data, they will still only pick out bright pixel values. Without loss of generality, the Weibull-based CFAR is used, and threshold  $T(i, j)$  at  $(i, j)$  for the search template is calculated by

$$T(i, j) = \frac{\sqrt{6}}{\pi} \{\lg[-\lg(P_{f_a})] + 0.5764\} \sigma_{ij} + \mu_{ij} \quad (15)$$

where  $P_{f_a}$  denotes the false alarm rate (FAR), and  $\mu_{ij}$  and  $\sigma_{ij}$  denote the mean and standard deviation of the pixel values in the tile being processed.

Because of the ship's superstructure, the filter-before-detect processing can improve the efficiency and get a good detection result  $I_2''$ .

### 2.3. Fusion Detection Algorithm

In this subsection, we advance the method of fusion processing for the detected images in order that we can get more accurate detection results. Let  $I$  denote the SAR image and pixel values  $I(i, j) \in [0, 1]$ . The SAR image  $I$  is used to obtain final result  $I_d$ .

The main steps of the ship detection algorithm based on manifold method are as follows:

Step 1: For implementation of the proposed algorithm based on curvature tensor of Gamma manifold, a square-shaped sliding window of  $h \times h$  pixels is used.

Step 2: For each image patch of  $I$ , with a size of  $h$ -by- $h$ , a Fisher metric matrix  $[g_{ij}]$  is constructed.

Step 3: For each image patch of  $I$ , with a size of  $h$ -by- $h$ , Riemannian curvature tensor  $R_{121}^2$  at position  $(i, j)$  is calculated.

Step 4: Reshape curvature tensors of surface into matrix  $I_1'$ . The OTSU method is implemented to locate ROIs, and the result is denoted by  $I_1''$ .

Step 5: SAR image  $I$  is filtered by using the nonlinear diffusion filtering method. The filtered image is denoted by  $I_2'$ . For implementation of the proposed algorithm based on surface manifold, the conductance parameter  $\eta$  and iteration parameter  $T$  are used.

Step 6: After filtering, the Weibull-based CFAR is used, and threshold  $T(i, j)$  at  $(i, j)$  for the search template is calculated by using Equation (15). We denote the result as  $I_2''$ .

Step 7: For the fusion processing, the final detected result  $I_d$  at position  $(i, j)$  is defined by  $I_d(i, j) = I_1''(i, j)I_2''(i, j)$ .

## 3. RESULTS AND DISCUSSION

### 3.1. Experimental Results

The ERS-1, 2 satellites are intended for global measurements of sea wind and waves, ocean and ice monitoring, coastal studies and land sensing using active and passive microwave remote sensing systems. The SAR image patch is shown in Fig. 2(a), with the size of  $150 \times 150$ . The data are C-VV. The pixel resolution is 30 meters in azimuth direction and 26.3 meters in range direction. An environmental satellite advanced SAR image patch near Hong Kong is shown in Fig. 2(b), with the size of  $150 \times 150$ . The data are C-VV. The pixel resolution is 4.1 meter in azimuth direction and 7.8 meters in range direction. Without loss of generality, they are used to assess the effectiveness of the proposed approach.

Because of the variations in ocean backscatter caused by variations in surface wind speed and direction, sea clutter impacts seriously on the effect and efficiency of maritime surveillance radars (as

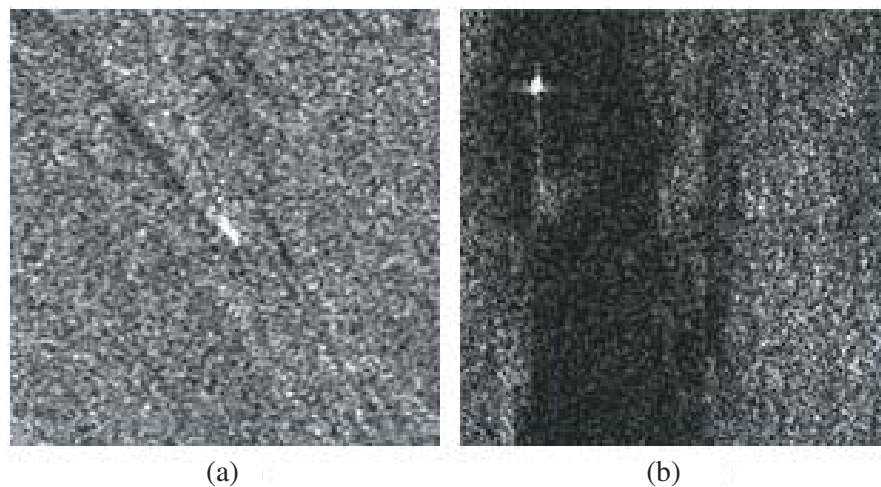


**Figure 2.** SAR image patches with a size of  $150 \times 150$  pixels.

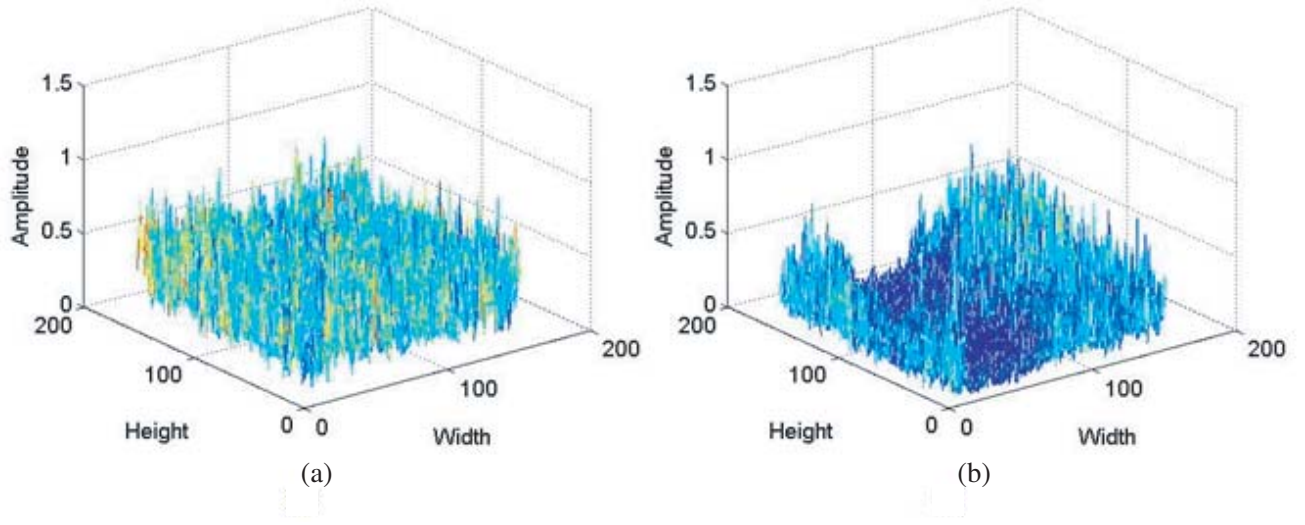


**Figure 3.** Mesh plots for the SAR image patches. (a) Fig. 2(a). (b) Fig. 2(b).

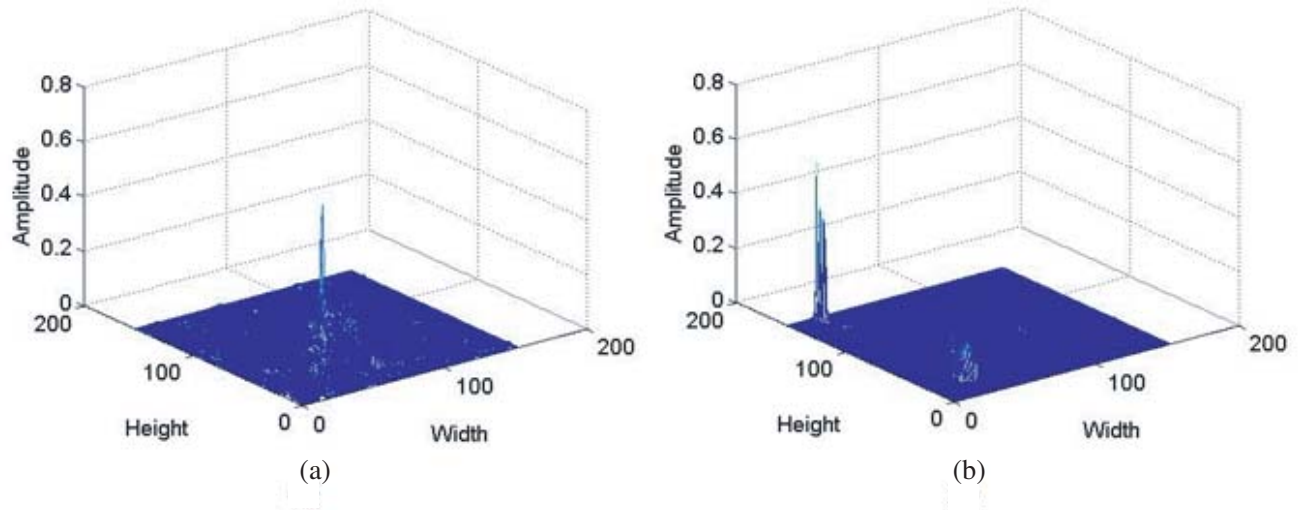


**Figure 4.** Normalized Riemannian curvature matrix  $I'_1$ . (a) Result of SAR image patch Fig. 2(a). (b) Result of SAR image patch Fig. 2(b).

shown in Fig. 3). Fig. 3 displays them with 3D scenes. This makes it harder to solve problems in ship detection that are causing stress for practical application.

During the experiments, the square-shaped sliding window is set as  $9 \times 9$  pixels. By using the maximum likelihood estimation method, the local parameters in the Gamma distribution are solved. We compute the normalized Riemannian curvature tensor matrix  $I'_1$  from the SAR images. From Fig. 4, the images  $I'_1$  can achieve a higher contrast between targets and background because of the ship superstructure. The OTSU method is implemented to locate ROIs, as shown in Fig. 5. From Fig. 5, the detected results are not satisfying because of the complicated situation of sea surface.

The key of image nonlinear diffusion filtering based on partial differential equations is to determine the appropriate diffusion mechanism and parameters. The parameters for nonlinear diffusion filtering are selected as follows: the time step size  $t = 5$ ,  $\eta = 10^{-13}$ ,  $\tau = 1.4$ ,  $\sigma = 1$ , and the number of iterations  $T = 10$ . The main goal of nonlinear diffusion filtering is to get the representation of smooth surface of SAR images. Fig. 6 shows the results of application. From Fig. 6, because of irregularly curved surface, the difference of the geometrical feature between artificial target and natural background is not

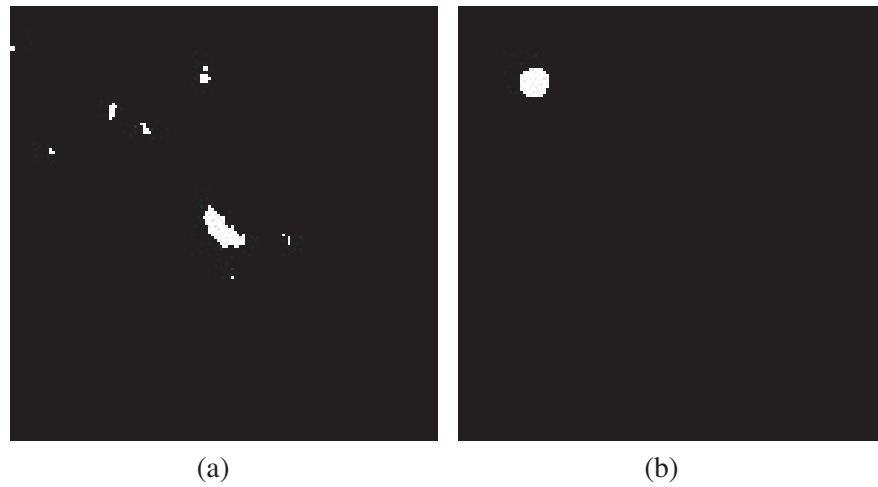


**Figure 5.** Results  $I_1''$  based on Gamma manifold and OTSU. (a) Result of SAR image patch in Fig. 2(a). (b) Result of SAR image patch in Fig. 2(b).

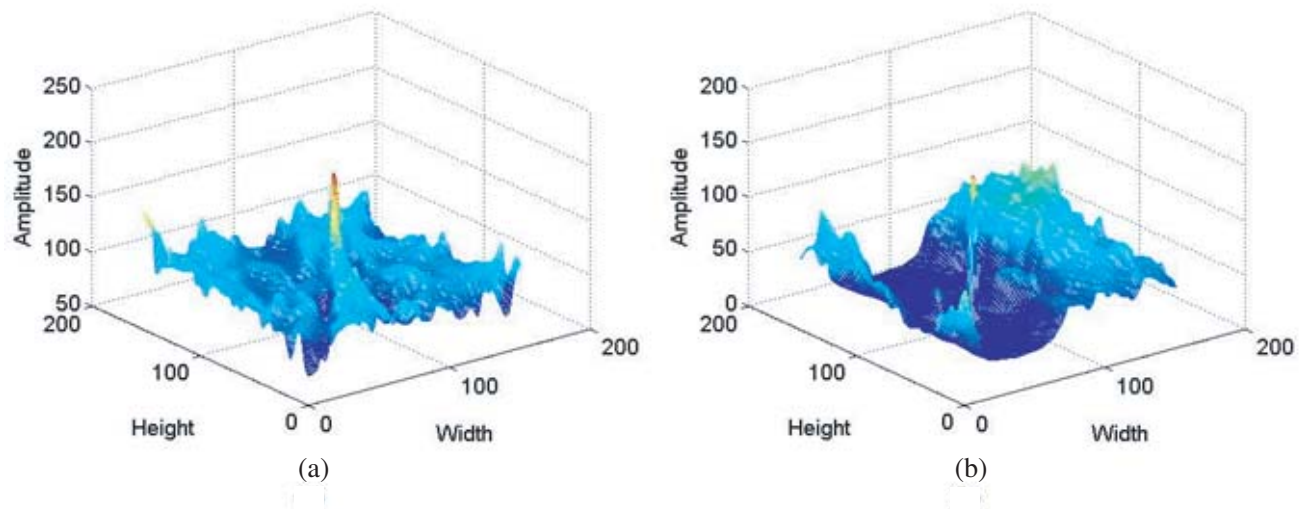


**Figure 6.** Filtered image patches by using nonlinear diffusion filtering. (a) Mesh plot for the SAR image patch as shown in Fig. 2(a). (b) Mesh plot for the SAR image patch as shown in Fig. 2(b).

obvious in the whole region. Some simple shape factors could not express differences between them in the filtered images. It is necessary to discuss the structure of neighbor of a planar point on a surface by using local adaptive threshold algorithms.

The CFAR-based method takes account of microstructure features of irregularly curved surface in the geometrical representation of SAR images. In this work, Weibull-based detector is adopted to achieve target detection. During the experiments, the square-shaped sliding window is set as  $25 \times 25$  pixels. The false alarm rate (FAR) is set as  $P_{fa} = 10^{-6}$ . To compare between Fig. 7(a) and Fig. 7(b), the same set of parameters may not be suitable for different complicated backgrounds of sea.

Figure 8 shows ROIs by using fusion processing. As shown in Fig. 8, the proposed scheme is highly efficient. It can both restrain the influence of the clutter and get perfect detection results for the SAR images.

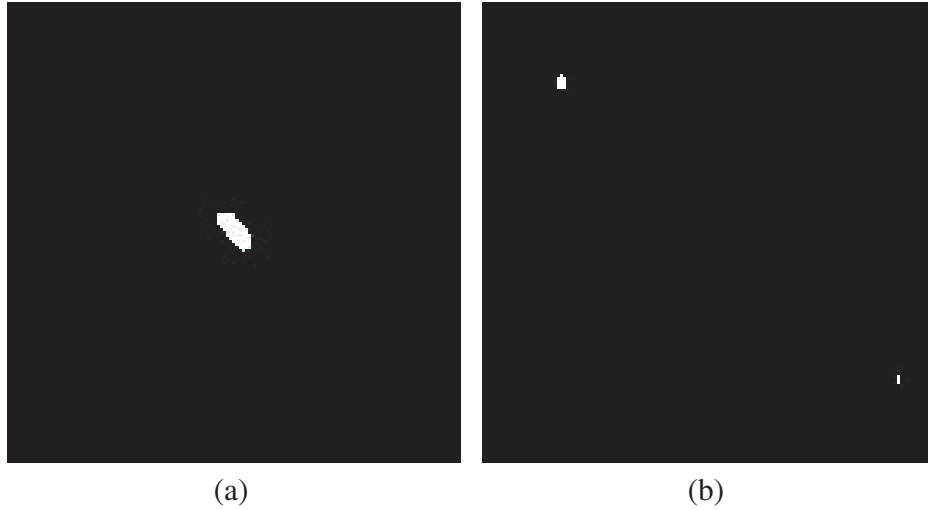


**Figure 7.** Results based on surface manifold and CFAR. (a) Result of SAR image patch in Fig. 2(a). (b) Result of SAR image patch in Fig. 2(b).

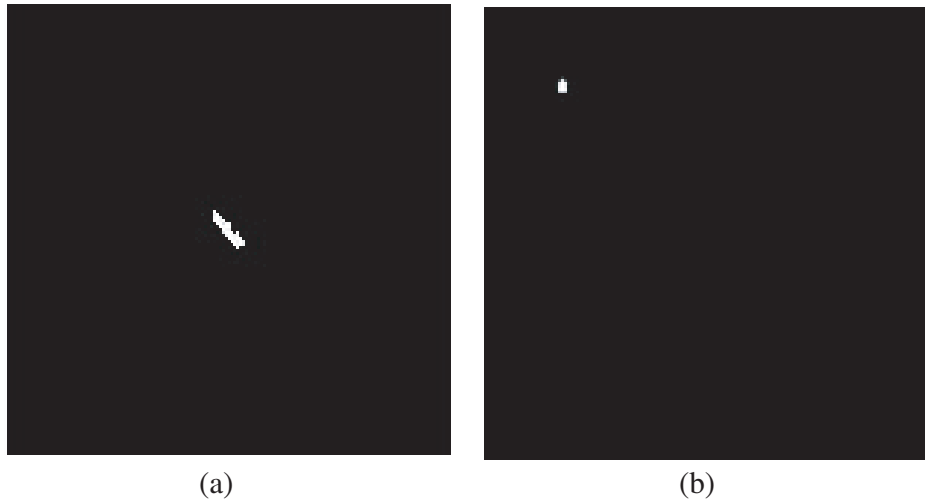


**Figure 8.** Fusion results. (a) Fusion Result of Fig. 5(a) and Fig. 7(a). (b) Fusion Result of Fig. 5(b) and Fig. 7(b).

### 3.2. Qualitative Discussion

SAR images show that the sea surface presents irregular performance and statistical self similarity, which means that each portion can be considered as a reduced scale image of the whole. This is the theoretical foundation that the statistic method of SAR image analysis is used. Information geometry emerged from the study of the geometrical structure of statistical manifold. It has been used to be applied to various fields of information sciences where probability statistics plays an important role. SAR imaging and processing is one of the major fields for information geometry applications.

For the processing of Gamma manifold in this work, we draw motivation from the information geometry for target classification problem. The core algorithm of this processing is the generation based on the higher contrast between ROIs and background. Therefore, ROIs can be separated from the background with the classic classification method.

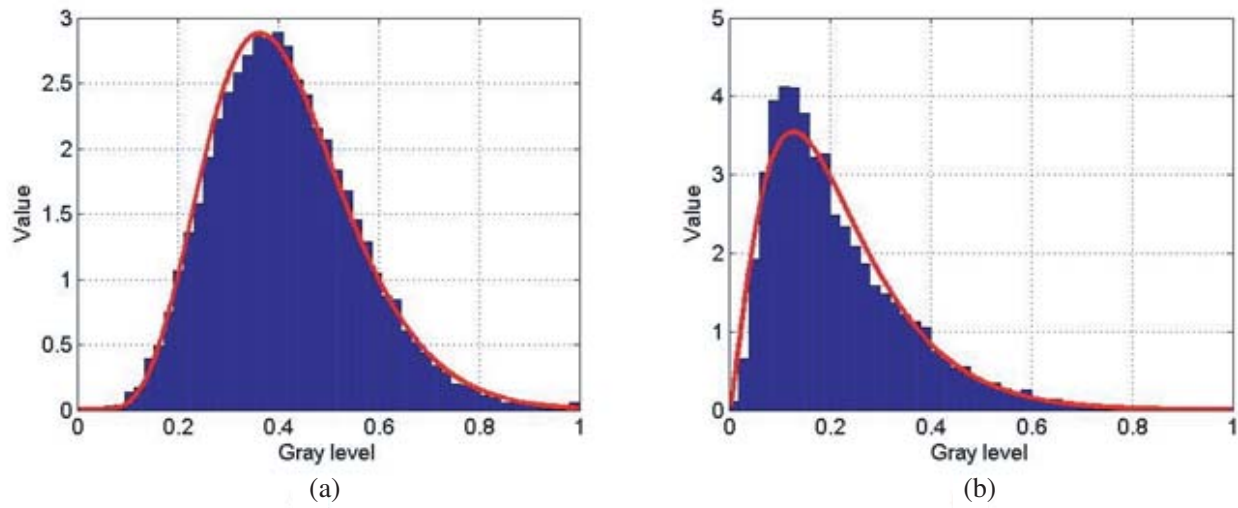


**Figure 9.** Histogram of clutter data shown in Fig. 2. (a) Result of SAR image patch in Fig. 2(a). (b) Result of SAR image patch in Fig. 2(b).

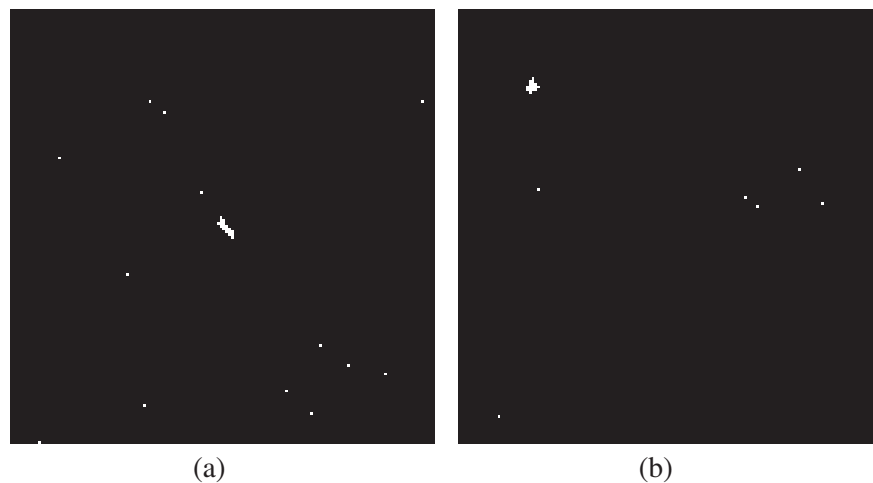


**Figure 10.** Detection results by using the Weibull-based CFAR detector with target window size  $25 \times 25$ . (a) Result of SAR image patch in Fig. 2(a). (b) Result of SAR image patch in Fig. 2(b).

As shown in Fig. 2 or Fig. 3, the images are corrupted by clutter. Fig. 9 shows the histogram of clutter data for images shown in Fig. 2 or Fig. 3. Because of the nonhomogeneity of sea clutter in the intensity domain, it is usually complicated to promote the accuracy of the distribution model to a very high level, which results in false alarm.

Figure 10 shows the detected-results by using the CFAR against Weibull clutter. It tends to have many false alarms by choosing design parameters, the false alarm rate (FAR)  $P_{f_a} = 10^{-6}$ . Because of the difficulty with the conventional adaptive threshold algorithms for ship detection, such as CFAR detectors, this article searches for new and better ways to detect ships in SAR images. The comparison between the proposed method and the CFAR-based method shows that the proposed method performs much better when the images are corrupted by clutter.

In summary, it is demonstrated that the proposed frame is effective. The proposed method can efficiently restrain the false alarm caused by incorrect statistical model and inaccurate parameter estimates. Therefore, it has potential application prospect in SAR image analysis.

#### 4. CONCLUSION

This article analyzes the problems in the ship detection from another point of view. Statistical manifolds represent smooth families of probability density functions, which allow information geometry to be applied to problems in target detection and representation of SAR images. Apart from statistic features, the detectability and identifiability of the ships depend also on the geometric structure of the surfaces in SAR images.

The proposed method could guarantee the differential geometric properties of families of certain distribution and surface of SAR images. The proposed fusion frame can achieve a good performance for inhomogeneous sea state, which has a great application value.

#### ACKNOWLEDGMENT

This study was supported in part by the National Natural Science Foundation of China (No. 61501152).

#### REFERENCES

1. Gao, G., S. Gao, J. He, and G. Li, "Ship detection using compact polarimetric SAR based on the notch filter," *IEEE Trans. Geosci. Remote Sens.*, Vol. 56, No. 9, 5380–5393, 2018.
2. Jiao, J., Y. Zhang, H. Sun, X. Yang, X. Gao, W. Hong, K. Fu, X. Sun, "A densely connected end-to-end neural network for multiscale and multiscene SAR ship detection," *IEEE Access*, Vol. 6, 20881–20892, 2018.
3. Li, T., Z. Liu, L. Ran, and R. Xie, "Target detection by exploiting superpixel-level statistical dissimilarity for SAR imagery," *IEEE Geosci. Remote Sens. Lett.*, Vol. 15, No. 4, 562–566, 2018.
4. Li, T., Z. Liu, R. Xie, and L. Ran, "An improved superpixel-level CFAR detection method for ship targets in high-resolution SAR images," *IEEE J. Sel. Topics Appl. Earth Observ.*, Vol. 11, No. 1, 184–194, 2018.
5. Odysseas, P., A. Alin, and B. David, "Superpixel-level CFAR detectors for ship detection in SAR imagery," *IEEE Geosci. Remote Sens. Lett.*, Vol. 15, No. 9, 1397–1401, 2018.
6. Ai, J., X. Yang, J. Song, Z. Dong, L. Jia, and F. Zhou, "An adaptively truncated clutter-statistics-based two-parameter CFAR detector in SAR imagery," *IEEE J. Oceanic Eng.*, Vol. 43, No. 1, 267–279, 2018.
7. Amari, S., *Information Geometry and Its Application*, Springer, Tokyo, 2016.
8. Nielsen, F. and R. Bhatia, *Matrix Information Geometry*, Springer-Verlag, Heidelberg, 2013.
9. Forbes, C., M. Evans, N. Hastings, and B. Peacock, *Statistical Distributions*, Wiley, New York, 2010.
10. Arwini, K. A. and C. T. J. Dodson, *Information Geometry — Near Randomness and Near Independence*, Springer-Verlag, Heidelberg, 2008.
11. Xue, J.-H. and D. M. Titterton, "T-tests, F-tests and Otsu's methods for image thresholding," *IEEE Trans. Image Process.*, Vol. 20, No. 8, 2392–2396, 2011.
12. Fabbrini, L., M. Greco, M. Messina, and G. Pinelli, "Improved edge enhancing diffusion filter for speckle-corrupted images," *IEEE Geosci. Remote Sens. Lett.*, Vol. 11, No. 1, 119–123, 2014.